Reaction kinetics of NO2 with liquid water at low particle pressures

ARTICLE *in* THE JOURNAL OF PHYSICAL CHEMISTRY · APRIL 1981

Impact Factor: 2.78 · DOI: 10.1021/j150607a022

2 AUTHORS, INCLUDING:

S. E. Schwartz
Brookhaven National Laboratory, Upton NY, …

231 PUBLICATIONS **9,681** CITATIONS

Reaction Kinetics of Nitrogen Dioxide with Liquid Water at Low Partial Pressure

Y.-N. Lee* and S. E. Schwartz

Environmental Chemistry Division, Department of Energy and Environment, Brookhaven National Laboratory, Upton, New York 11973
(Received: October 17, 1980)

The reaction $2NO_2(g) + H_2O(l) \rightarrow 2H^+ + NO_3^- + NO_2^-$ (1) has been studied for $1 \times 10^{-7} \leq p_{NO_2} \leq 8 \times 10^{-4}$ atm. Since this reaction involves the transfer of a reactant from the gas into the aqueous phase, the rate depends upon the following: (a) physical mass transfer of the reactant, (b) the equilibrium solubility of NO_2, and (c) homogeneous aqueous-phase kinetics. In order for the observed rate to yield information most sensitive to (c), the rate of (a) must be comparable to that of (c). In the case of a second-order reaction, this can be achieved by working at low partial pressure of NO_2 as well as a high rate of physical mixing of the two phases. To facilitate the latter, the gas was brought into contact with the liquid as finely dispersed bubbles produced by flowing through a disk-frit; the mass transfer time constant, determined by uptake of CO_2, was τ_m = 1.7–5.3 s. The rate of reaction 1, monitored by observing the electrical conductivity of the aqueous solution, exhibited dependence on p_{NO_2} and τ_m consistent with second-order kinetics and a steady-state aqueous-phase NO_2 concentration. Values of H_{NO_2}, the Henry's law coefficient, and k_1, the second-order aqueous-phase rate constant, were determined to be $(7.0 \pm 0.5) \times 10^{-3}$ M atm^{-1} and $(1.0 \pm 0.1) \times 10^8$ M^{-1} s^{-1}, respectively, at 22 °C. Self-consistency of the gas–liquid reaction model has been demonstrated in terms of the identity of the diffusing species and the extent of mass-transport limitation.

Introduction

Because of its thermodynamic stability, nitric acid is an important sink for nitrogen oxides in the atmosphere.[1,2] Consequently, knowledge of the rate and mechanism of formation of HNO_3 from its precursors is important in the description of atmospheric chemistry of the nitrogen oxides, including the incorporation of these species into clouds and precipitation in the ambient atmosphere. Although substantial understanding of the homogeneous gas-phase processes leading to HNO_3 formation has now been attained,[2] comparatively little attention has been given to the corresponding heterogeneous processes. Among these, the reaction of NO_2 with liquid water to form nitric and nitrous acids, reaction 1, would appear, on the

$$2NO_2(g) + H_2O(l) \rightarrow 2H^+ + NO_3^- + NO_2^- \qquad (1)$$

basis of equilibrium considerations,[3,4] to be an important pathway. However, present knowledge of the physical solubility of NO_2 (Henry's law coefficient) and of the aqueous-phase kinetics of reaction 1 appears inadequate to permit confident evaluation of the rate of this process in the ambient atmosphere.

The kinetics of reaction 1, which is the rate-determining step of the industrially important process of nitric acid manufacture,[5] has been investigated by a wide variety of techniques. These include indirect studies via the kinetics of nitrous acid formation and decomposition[6,7] and studies of the aqueous-phase reaction by pulse radiolysis and flash photolysis,[8,9] as well as direct measurements of the rate of absorption of NO_2 and/or N_2O_4 into liquid water.[10-12] These studies have recently been reviewed elsewhere.[13]

Unfortunately, despite the abundant research on the kinetics of this reaction, information requisite to describe this reaction under conditions of atmospheric interest is still lacking. The reasons are twofold. First, the studies that have been conducted pertain to partial pressures of NO_2 that are higher by at least three to five orders of magnitude than those characteristic of the ambient atmosphere. Consequently, it is impossible to exclude mechanisms potentially important in the low-pressure region that would be masked at higher pressures by processes that are higher order in NO_2. Secondly, despite numerous studies, there remain substantial discrepancies (as much as an order of magnitude) in such critical quantities as Henry's law coefficients and rate constants in this system.[13]

TABLE I: Mixing Conditions for Limiting Regimes of Gas-Liquid Reactions[a]

regime	condition
phase mixed	$\tau_r \gtrsim 10\tau_m$ or $\tau_r \gtrsim 10\tau_d$
convective mass-transport controlled	$\tau_m \gtrsim 10\tau_r$, $\tau_r \gtrsim 3\tau_m^2/\tau_d$
diffusive mass-transport controlled	$\tau_d \gtrsim 10\tau_r$, $\tau_r \lesssim 0.38\tau_m^2/\tau_d$

[a] τ_r, τ_m, and τ_d are the characteristic time of reaction, convective mixing, and molecular diffusion, as defined by $\tau_r = \{(-d_r[A]/dt)/[A]\}^{-1}$, $\tau_m = (k_L a)^{-1}$, and $\tau_d = (Da^2)^{-1}$, respectively. In these equations a is the interfacial area per unit liquid volume, D is the aqueous-phase diffusion coefficient of dissolved species A, and k_L is the liquid-side mass transfer coefficient as illustrated in the Appendix.

(1) E. Robinson and R. C. Robbins, *J. Air Pollut. Control Assoc.*, **20**, 303 (1970).
(2) D. L. Baulch, R. A. Cox, R. F. Hampson, Jr., J. A. Kerr, J. Troe, and R. T. Watson, *J. Phys. Chem. Ref. Data*, **9**, 295 (1980).
(3) A. E. Orel and J. H. Seinfeld, *Environ. Sci. Technol.*, 11, 1000 (1977).
(4) S. E. Schwartz and W. H. White, *Advan. Environ. Sci. Eng.*, in press.
(5) T. H. Chilton, "Strong Water", the M.I.T. Press, Cambridge, MA, 1968.
(6) (a) E. Abel and H. Schmid, *Z. Phys. Chem.*, **134**, 279 (1928); (b) E. Abel, H. Schmid, and S. Babad, *ibid.*, **136**, 135 (1928); (c) E. Abel, H. Schmid, and E. Römer, *ibid.*, **148**, 337 (1930).
(7) H. Komiyama and H. Inoue, *J. Chem. Eng. Jpn.*, 11, 25 (1978).
(8) M. Grätzel, A. Henglein, J. Lilie, and G. Beck, *Ber. Bunsenges. Phys. Chem.*, **73**, 646 (1969).
(9) A. Treinin and E. Hayon, *J. Am. Chem. Soc.*, **92**, 5821 (1970).
(10) S. P. S. Andrew and D. Hanson, *Chem. Eng. Sci.*, **14**, 105 (1961).
(11) H. Komiyama and H. Inoue, *Chem. Eng. Sci.*, **35**, 154 (1980).
(12) H. Kramers, M. P. P. Blind, and E. Snoeck, *Chem. Eng. Sci.*, **14**, 115 (1961).
(13) S. E. Schwartz and W. H. White, manuscript in preparation.

0022-3654/81/2085-0840$01.25/0

TABLE II: Apparent Reaction Order with Respect to NO_2 for Limiting Regimes as a Function of True Aqueous-Phase Reaction Order (Diffusing Species NO_2)

reaction order	phase mixed	convective mass transport	diffusive mass transport
0	0	1	1/2
1	1	1	1
2	2	1	3/2
m	m	1	$m/2 + 1/2$

Increasing Reaction Rate →

TABLE III: Apparent Reaction Order with Respect to NO_2 for Limiting Regimes as a Function of True Aqueous-Phase Reaction Order (Diffusing Species N_2O_4)

reaction order	phase mixed	convective mass transport	diffusive mass transport
0	0	2	1
1	1	2	3/2
2	2	2	2
m	m	2	$m/2 + 1$

Increasing Reaction Rate →

The present study was directed to a determination of the physical solubility of NO_2 and the aqueous-phase rate coefficient of reaction 1 at concentrations corresponding to ppm and sub-ppm partial pressures of NO_2, by direct measurement of the rate of reactive dissolution of NO_2 into water. These quantities may be determined from experiments conducted in a gas–liquid reactor for which the rate of mixing of the two phases is quantitatively characterized.

Theory

Apparent Reaction Order. The rate of a gas–liquid reaction depends upon the physical solubility of the reactant gas, the rate of mass transport of the reactant, and aqueous-phase reaction kinetics. Depending on the rate and mechanism of mass transport relative to the rate of reaction, such reactions may be distinguished into three regimes: (1) molecular diffusion controlled; (2) convective mass-transport controlled; and (3) phase mixed. The criteria for establishing the regime that pertains to a given reaction system under examination have been discussed extensively (e.g., ref 14) and are summarized in Table I; however, for a system of unknown reaction kinetics and mechanism, these criteria are not immediately applicable. Rather, it is necessary to infer the regime on the basis of observation (e.g., the power-law dependence of the rate of reaction upon the partial pressure of the reactant gas, i.e., the "apparent reaction order") and subsequently to confirm the self-consistency of the interpretation. In Table II we have displayed the apparent reaction order for various actual reaction orders for each of the several regimes. It should be emphasized that the regimes must be viewed as limiting cases and that intermediate situations, and in turn intermediate observed reaction orders, would be expected. Thus, one should approach such an interpretation with caution.

In the case of aqueous-phase reaction of NO_2, one has an additional complexity arising from association to form the dimer N_2O_4. This association occurs not only in the gas phase, but also (and of relevance to the present study) in the aqueous phase.[8,9] Since the apparent reaction order relative to p_{NO_2} depends on the competition between mass transport and chemical reaction, it can be influenced by whether the principal aqueous-phase diffusing species is NO_2 or N_2O_4. This effect is illustrated in Table III, in which is shown the apparent reaction order with respect to $NO_2(g)$, evaluated for the several limiting cases under the assumption that the principal aqueous-phase diffusing species is N_2O_4, rather than NO_2. It is seen that the identity of the diffusing species affects the apparent reaction order in both the diffusive and convective regimes. Despite this complexity, examination of the apparent reaction order with respect to p_{NO_2} nevertheless remains a principal means of discerning the aqueous-phase reaction mechanism and the identity of the diffusing species.

Slow Reaction Model. Although the dependence of the rate of reaction upon gas-phase partial pressure of the reagent is difficult to treat for intermediate regimes, one case that is amenable to such treatment is that of so-called "slow" reactions, i.e., situations intermediate between the phase-mixed and convective mass-transport controlled regimes. In this regime, the reaction is considered to occur in the "bulk", the aqueous-phase reagent concentration being controlled by competition between convective mass transport and chemical reaction. Denoting the reagent as A, one has the processes

$$A_s \xrightarrow{k_m} A_a$$

$$A_a \xrightarrow{k_{-m}} A_s$$

$$2A_a \xrightarrow{k_l} \text{products}$$

where $k_m = k_{-m}$ are stochastic rate coefficients for convective mixing (conventionally denoted as $k_L a$ in the chemical engineering literature, e.g., ref 14), k_l is the rate coefficient for aqueous phase reaction, and the subscripts s and a denote surface and bulk aqueous concentrations, respectively. (Here a reaction stoichiometry of 2 is explicitly assumed, but the reaction order is left as a parameter of the model, i.e., $d[A]/dt = -2k_l[A]^n$.) According to this model the surface concentration is assumed to be in phase equilibrium with the interfacial gas-phase partial pressure of the reagent gas, i.e., $[A_s] = Hp$, and the bulk reagent concentration is assumed to be uniform.[14] Assuming steady state one obtains the following equation for $[A_a]$:

$$2k_l[A_a]^n + k_m[A_a] - k_m Hp = 0 \qquad (2)$$

which may be solved for $[A_a]$, in order to yield the expression for the rate $R_l = k_l[A_a]^n$. For a first-order reaction ($n = 1$)

$$[A_a] = \frac{k_m Hp}{k_m + 2k_l}$$

and hence

$$R_l = \frac{k_l Hp}{1 + 2k_l\tau_m} \qquad (3)$$

Likewise for a second-order reaction ($n = 2$)

$$[A_a] = \frac{(1 + 8\tau_m k_l Hp)^{1/2} - 1}{4\tau_m k_l}$$

which gives

$$R_l = \frac{1}{2\tau_m}\left\{Hp + \frac{1}{4\tau_m k_l}[1 - (1 + 8\tau_m k_l Hp)^{1/2}]\right\} \qquad (4)$$

In these expressions τ_m is the convective mixing time constant (k_m^{-1}).

(14) P. V. Danckwerts, "Gas-Liquid Reactions", McGraw-Hill, New York, 1970.

Equation 2 also gives the appropriate limits for when the rate of reaction is much smaller or much greater than that of phase mixing, viz.

$$R_l = k_l H^n p^n \qquad 2k_l[A_a]^n \ll k_m[A_a] \tag{5}$$

corresponding to the phase-mixed regime, and

$$R_l = k_m H p/2 \qquad 2k_l[A_a]^n \gg k_m[A_a] \tag{6}$$

corresponding to the convective mass-transfer-controlled regime.

Equations 3–6 serve to point out an important advantage of studying gas–liquid reactions in the slow reaction regime. Thus it may be seen that experiments conducted in the phase-mixed regime are capable of yielding only the product $H^n k_l$, and, conversely, that experiments in the convective mass-transport regime can yield only H, assuming a known k_m. However, by conducting experiments within the intermediate range it should be possible, by varying k_m, to determine both H and k_l.

Experimental Section

On the basis of the preceding discussion it was considered advantageous to carry out the experimental measurement of the rate of reactive dissolution of NO_2 into water in a reactor which permits the mixing time constant τ_m to be varied and calibrated. In addition, the values of τ_m and τ_r should be comparable and should be maintained unchanged throughout the course of a given run. The reactor which was designed to meet these objectives consisted of a cylindrical vessel with a fritted disk as the bottom surface, through which the gaseous reagent was introduced as finely divided bubbles. This means of introducing the gas both provided a large interfacial area and served to promote convective mixing as induced by the upward motion of the bubbles. A constant reagent concentration was maintained by continuously replenishing the reagent by using a once-through flow. The rate of reaction was determined by the cumulation of the products in the solution.

In view of the ionic nature of the products, electrical conductivity was selected as a convenient, continuous measure of the extent of reaction. The requirement of maintaining the rate of reaction comparable to that of convective mixing was furthered by employing low partial pressures of NO_2, since, for a second-order reaction, this rate will be inversely proportional to the aqueous phase NO_2 concentration. Determination of the mixing time (τ_m) of the reactor was achieved with the use of CO_2, as described in the Appendix.

Materials. Stock cylinders of NO_2 at concentrations of 9.1 and 99 ppm (±1%), in N_2, were obtained from Scott Environmental Technology, Inc. as certified Acublend master gases. A stock cylinder 800 ppm of NO_2 in air was obtained from Airco (Spectra-seal grade). NO_2 concentrations of these gases were intercompared with each other and with two other independent standards: i.e., 5.14 ppm of NO in N_2 (Scott), and a NO_2 permeation tube (Monitor Labs, 225 ng/min at 50 °C). The several sources were found to be mutually consistent in NO_2 concentration within 5% as ascertained both by NO chemiluminescence (REM, Model 642A) and Saltzman colorimetric determination.[15]

Diluent gas N_2, of ultrahigh purity (99.999%), was supplied by either Matheson or Liquid Carbonic. It was passed through BASF catalyst R3-11 (obtained from Chemical Dynamic Co.) containing highly dispersed activated copper to remove any trace amount of oxidant, e.g., O_2. The water employed as reagent and for humidification of the diluent gas was of reagent grade (type I, ASTM) and has been purified by a Millipore Milli-Q water system; the specific resistance of the water thus purified was consistently greater than 16 Mohm cm^{-1} at 25 °C.

Reagent grade inorganic salts, KCl, KNO_3, and $NaNO_2$ (Fisher Co.), were used without further purification. Bone dry CO_2 (99.8%, Matheson) was used in the characterization of the mixing time constant of the reaction cell.

Reaction Cell. The all-glass reaction cell equipped with a water jacket for temperature control is depicted in Figure 1. Gas is brought into contact with the liquid as finely dispersed bubbles by flowing through a coarse porosity frit-disk fused to the cylindrical cell wall. To prevent loss of water as small droplets, two baffles were attached at the top of the cell near the gas exit. When the incoming gas was prehumidified (see below), the amount of liquid in the cell remained essentially unchanged after 2 h of bubbling.

Thermostatted water regulated to within ±0.1 °C was circulated through the water jacket in order to maintain a constant temperature of the reaction cell. The temperature of the cell was monitored by a thermistor placed in the temperature well. For the experiments reported here a constant temperature of 22.0 ± 0.1 °C was employed.

Conductivity Measurement. The electrical conductivity of the solution was measured by means of Pt electrodes introduced into the cell via leads fused into a detachable ground glass plug (Figure 1). It was found that the

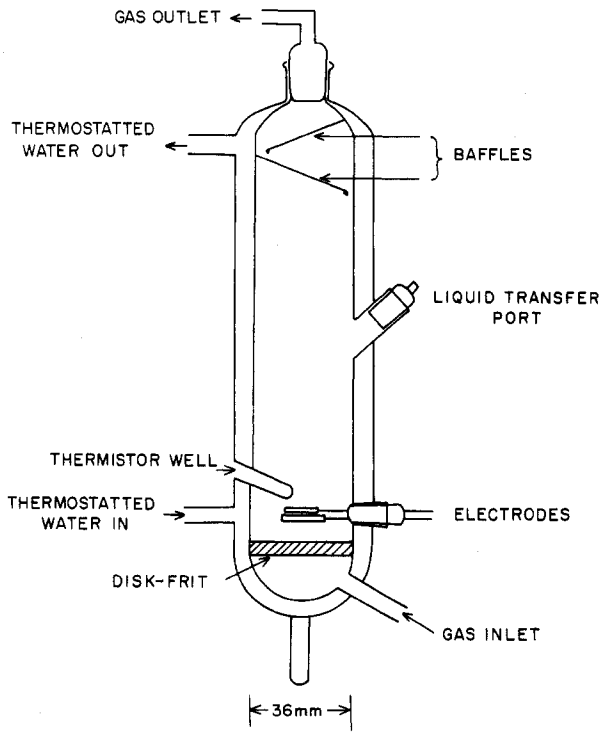

Figure 1. Gas–liquid reaction cell.

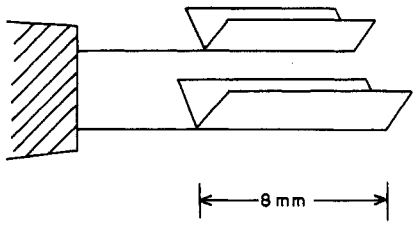

Figure 2. Platinum electrodes for the conductivity measurement.

(15) B. E. Saltzman, *Anal. Chem.*, **26**, 1949 (1954).

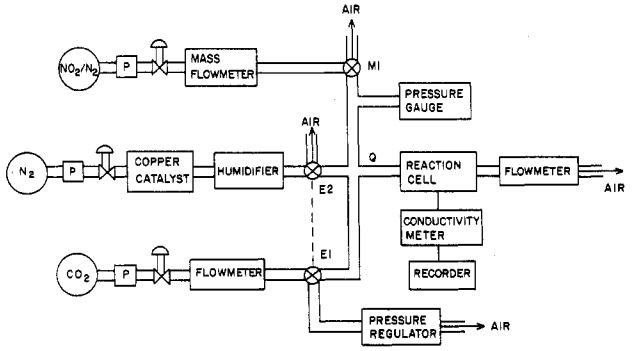

Figure 3. Schematic of the experimental setup. E1 and E2 are electrically coupled solenoid valves.

presence of gas bubbles near or between the electrodes complicated the measurement since they effectively diminished the cell constant. This problem was minimized by arranging the two electrode plates horizontally, with the lower one slightly larger than the upper. Bending the plates into a V shape (Figure 2) was observed to further decrease the noise introduced by the random passage of bubbles between the plates. For volumes less than 30 mL and total gas flow rate less than 2 L/min the "noise" in the cell constant was typically smaller than 4%. Determination of the cell constant was achieved by standards of known concentration (e.g., KNO_3, HCl). Approximate dimensions of the electrodes were 8 × 8 mm with a spacing approximately 3 mm. When the reaction cell contained at least 30 mL of water, the gas bubbles were sufficiently sparse in the region of the electrodes that the effective cell constant was identical with that represented by physical geometry of the electrodes. At lower liquid volumes the cell constant was somewhat lower; at a gas flow rate of 2.0 L/min the ratio of the effective cell constant to that determined by physical geometry was 0.99 and 0.87 (±1%) at 15 and 10 mL, respectively.

An ac conductivity meter (Electromark 4401, 12 kHz) was employed, yielding a sensitivity with these electrodes of 0.01 μmho cm^{-1}, corresponding to 2×10^{-8} M HNO_3. The resulting conductivity measurements were recorded by a strip-chart recorder.

Reaction System Setup. The gas flow system is schematically illustrated in Figure 3. Stainless steel filters, designated as P (Matheson Model 6184), were employed to remove particulate matter (99.997% efficiency for size ≥0.03 μm). The humidifiers for the diluent gas, N_2, consisting of bubblers with fritted gas dispersion tubes immersed in high-purity water were located within the constant temperature bath. Stock NO_2 was mixed with the purified N_2 at point Q before entering the cell. Total flow rate was measured by a "rotameter" located at the exhaust of the reaction cell; the flow of stock NO_2 was measured by a mass flow meter (Matheson Model 8110). The gas entering the cell was nearly saturated with water vapor since the stock NO_2 flow was generally less than 10% of the total flow. Consequently, the total flow could be maintained relatively constant while NO_2 was switched on and off (by three-way valve M1). For experiments with high partial pressures of NO_2 (up to 800 ppm), dilution by N_2 sometimes was eliminated. In these experiments the evaporation loss of water from the reaction cell due to the dry incoming gas was negligible because of the short reaction time.

Procedure. In a typical run, a constant flow (e.g., 2.0 L/min) of N_2 was initially allowed to flow through the system, building up a slightly positive pressure upstream to the glass frit of the reaction cell (pressure drop across the frit was approximately 0.7 psi). After careful rinsing of the cell, a predetermined amount of water (between 10 and 70 mL) was introduced. The conductivity of the fresh charge of water, initially ~0.7 μmho cm^{-1}, decreased to ~0.06 μmho cm^{-1} in 5–10 min depending on the liquid volume; this decrease presumably reflects the degassing of CO_2 as a result of N_2 purging, since the initial conductivity is close to that expected for pure water saturated with atmospheric CO_2.

After the conductivity of the water became steady for 10–15 min the reaction was initiated by switching stock NO_2 gas into the system (valve M1). In order to achieve a constant flow with a stable NO_2 concentration (as monitored by a NO chemiluminescent detector) we found it necessary to maintain the NO_2 flow for at least 1 h prior to the reaction (to exhaust through valve M1).

Product Analysis. To complement the nonspecific conductivity method used in the kinetic study, the concentration of the reaction products was determined colorimetrically at the conclusion of experimental runs by azo dye formation from NO_2^-.[16] The amount of NO_3^- was measured by the same method after reduction to NO_2^- by hydrazine sulfate.[17]

Results

Product Analysis and Stoichiometry. The ratio of the concentrations of product NO_2^- and NO_3^- was in almost all instances found to be unity within analytical precision (typically 5%). This result was not affected by the reagent concentrations, mixing characteristics, and the length of the reaction time. The concentrations of the products, invariably less than 2×10^{-6} M, were in good agreement with those anticipated from the conductivity measurements, and were found to be stable for at least 24 h.

The partial pressure of NO_2 in the reactant gas was determined before and after passage through the reaction cell. The decrease in p_{NO_2} of ≲2% due to reaction was consistent with the observed rate of product formation and was sufficiently small for the p_{NO_2} to be taken as constant. These results establish that the stoichiometry of reactive dissolution of NO_2 at these partial pressures is that of reaction 1.

Reaction Rate Determination. During the reaction the specific conductivity, κ, of the solution was found to increase linearly with time. The reaction rate R_1, defined as

$$R_1 = d[HNO_3]/dt$$

can be determined from $d\kappa/dt$, using the limiting equivalent conductivities of H^+, NO_2^-, and NO_3^- at 22 °C.[18]

In order to examine the dependence of the reaction rate on p_{NO_2}, we made rate measurements for partial pressure of NO_2 varying from 1×10^{-7} to 8×10^{-4} atm. A constant mixing condition was maintained, i.e., liquid volume of 10 mL and total gas flow of 2.0 L/min. (These conditions corresponded to a time constant for convective mixing τ_m = 1.69 s, as discussed below.) The experimental results are displayed in Figure 4.

To determine the physical quantities of interest (i.e., H_{NO_2} and k_1) we also examined the rate of reactive dissolution as a function of mixing conditions. These results, which cover $1 \times 10^{-7} \leq p_{NO_2} \leq 1 \times 10^{-5}$ atm, are given in

(16) L. J. Kamphake and R. T. Williams, "Automated Analysis for Environmental Pollution Control", Technicon Corporation, Ardsley, NY, 1973.

(17) L. J. Kamphake, S. A. Hannah, and J. M. Cohen, *Water Res.*, 1, 205 (1967).

(18) R. A. Robinson and R. H. Stokes, "Electrolyte Solutions", Academic Press, New York, 1959.

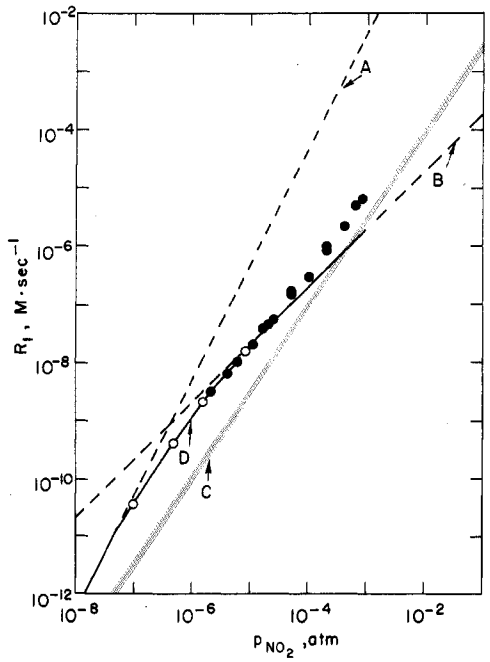

Figure 4. Dependence of the rate of reaction 1 upon p_{NO_2} at fixed mixing condition (k_m = 0.59 s^{-1}). Phase-mixed (line A), convective-mass-transport limited (line B), molecular diffusive controlled (zone C), and slow reaction regime (curve D) were calculated by using H_{NO_2} = 7.0 × 10^{-3} M atm^{-1}, k_l = 1.0 × 10^8 M^{-1} s^{-1}, and k_m, for a second-order reaction and NO_2 as the diffusant. Open points represent averages of four or more measurements.

TABLE IV: Rate of Reaction 1 Tabulated as a Function of p_{NO_2} and Characteristic Mixing Time τ_m

$10^6 p_{NO_2}$, atm	9.71	1.66	0.490	0.104
	R_l, M s^{-1}			
τ_m, s	× 10^8	× 10^9	× 10^{10}	× 10^{11}
1.69	1.73 (4%)[a]	2.08 (1%)	4.18 (5%)	3.83 (2%)
2.14	1.34 (2%)	1.66 (6%)	3.59 (1%)	3.53 (6%)
3.17	0.92 (2%)	1.22 (4%)	2.68 (1%)	3.01 (4%)
4.27	0.73 (3%)	0.98 (2%)	2.01 (3%)	2.38 (4%)
5.26	0.58 (1%)	0.82 (5%)	1.75 (4%)	2.04 (2%)

[a] Standard deviation, based typically on 4–6 measurements.

Table IV. In order to interpret these results, it was necessary to determine the mixing time constant τ_m for the various conditions (liquid volume, gas-flow rate) employed. This determination was achieved by the use of CO_2; the measurement methodology and results are given in the Appendix, as well as the justification of the use of CO_2 as a model appropriate to the uptake of NO_2 under the conditions of this experiment.

Gas-Phase Contribution. Examination was made to ascertain whether the observed product cumulation in the liquid of the reactor was due to entrainment of soluble gases either present as an impurity in the starting NO_2 stock gases, or produced by the gas-phase reaction $2NO_2 + H_2O \rightarrow HNO_3 + HNO_2$ (1G) prior to entering the reaction cell. To test the former possibility, we passed the reactant gas through a water-filled bubbler placed in between the mixing point Q and the reactor, which would remove any soluble gas. The rates measured with and without the scrubber showed no detectable difference, thus excluding the possibility that a soluble gas impurity was responsible for the observed rate. To examine the importance of reaction 1G, we increased the volume between the mixing point Q and the reactor from ~10 to ~300 mL by connecting a cylindrical glass tube between them. Again no change (≤2%) in apparent reaction rate was detected, therefore establishing that the gas-phase contribution is unimportant.

Discussion

The experimental results shown in Figure 4 display a power dependence of the reaction rate on p_{NO_2} of approximately 3/2, although careful examination of these data reveals small but a definite variation about such a value. It is tempting to infer the true reaction order and the identity of the diffusing species from this plot. However, examination of the pressure dependence alone is of limited value, because the apparent order with respect to p_{NO_2} depends upon the mass-transport regime that obtains and the identity of the diffusing species, in addition to the true reaction order. A complex relationship between these several "dimensions" can be seen from Table II and III, and it is clear that more than one situation might account for the apparent reaction order observed in Figure 4. Nevertheless, the apparent reaction order with respect to p_{NO_2} remains useful for comparison to predictions calculated from values of H_{NO_2}, k_l, and n that are determined by other approaches, e.g., study of the slow reaction regime.

In order to apply the equations of the slow reaction regime, it is necessary to establish that the conditions under which those equations are derived are met. First, the diffusing species was assumed to be NO_2 in the derivation. In the estimation of the ratio of $[N_2O_4]_a/[NO_2]_a$ for a given p_{NO_2}, one needs the knowledge of both H_{NO_2} and K_A, the aqueous-phase equilibrium constant for $2NO_2 \rightleftarrows N_2O_4$. The latter has been determined as 6.5 × 10^4 M^{-1} by Grätzel et al.[8] and the former was taken as H_{NO_2} = (1.2 ± 0.4) × 10^{-2} M atm^{-1}, as recommended by Schwartz and White on the basis of thermochemical cycles.[4] According to these values, the ratio of N(IV) present as N_2O_4 to that as NO_2, $N_{N_2O_4}/N_{NO_2}$, is estimated to be less than 0.02 at p_{NO_2} = 1 × 10^{-5} atm, and correspondingly less at lower p_{NO_2}, thus giving support to the assumption that NO_2 is the diffusing species.

The second requirement for the slow reaction regime is that

$$\tau_r \approx \tau_m$$

i.e., that the rate of convective mixing be of the same order of magnitude as that of chemical reaction. For values of τ_m = 1.7–5.3 s, the characteristic reaction time defined as

$$\tau_r = (2R_l/[NO_2]_a)^{-1}$$

will satisfy the condition, $\tau_r \approx \tau_m$, when the observed $R_l/p_{NO_2} \approx 0.06$–0.6 M s^{-1} atm^{-1}, and again assuming H_{NO_2} = 1.2 × 10^{-2} M atm^{-1}.

Based upon these considerations, we restrict the subsequent analysis to rate data obtained for $p_{NO_2} \leq 10^{-5}$ atm, as given in Table IV and in Figure 4. It has to be emphasized that the values of H_{NO_2} and K_A employed here are only tentative and have no quantitative influence on the analysis except for the fact that they qualitatively set the conditions for data range to be utilized. The determined quantities of interest will be subject to test for self-consistency.

Homogeneous Aqueous-Phase Kinetics and Reaction Order. Having tentatively established the appropriateness of the slow reaction treatment, we proceed to establish the reaction order. For a first-order reaction it is convenient to plot the results as a function of τ_m according to the rearranged form of eq 3.

$$\left(\frac{R_l}{p_{NO_2}}\right)^{-1} = \frac{1}{k_l H_{NO_2}} + \frac{2}{H_{NO_2}}\tau_m \qquad (7)$$

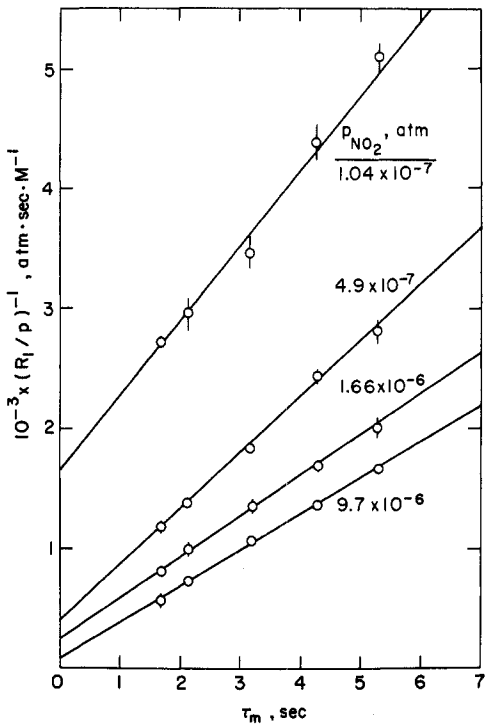

Figure 5. Dependence of the rate of reaction 1 upon characteristic mixing time, τ_m, plotted for a first-order reaction (eq 7), for indicated partial pressures of NO_2.

Equation 7 predicts a linear relation which should give the values of the two parameters k_1 and H_{NO_2} from the intercept and slope. Furthermore, these quantities are expected to be independent of the NO_2 partial pressure. It is clear from Figure 5 that the data, when plotted according to eq 7, although showing apparently straight lines for each of the several values of p_{NO_2} studied, do not exhibit the same slope and intercept as p_{NO_2} is varied. First-order aqueous-phase kinetics can therefore be excluded based on this argument.

To treat second-order kinetics, eq 4 may be rearranged into a convenient form for graphically displaying the data as

$$\left(\frac{R_1}{p_{NO_2}^2}\right)^{-1} = \frac{1}{k_1 H_{NO_2}^2}\left\{\frac{1}{2x} + \frac{1}{8x^2}[1 - (1 + 8x)^{1/2}]\right\}^{-1} \tag{8}$$

where $x = H_{NO_2} k_1 \tau_m p_{NO_2}$. In Figure 6 are shown the experimental data plotted in this manner. Again, there are two adjustable parameters, H_{NO_2} and k_1, which may be determined by a fit of the functional form (8) to the experimental data. This procedure leads to a satisfactory fit to the data for values of the two parameters $H_{NO_2} = (7.0 \pm 0.5) \times 10^{-3}$ M atm^{-1} and $k_1 = (1.0 \pm 0.1) \times 10^8$ M^{-1} s^{-1}. This fit to eq 8 is valid for the argument $\tau_m p_{NO_2}$ varying by more than two orders of magnitude, as indicated by the solid curve in Figure 6. The uncertainities associated with the fitted parameters were estimated from extreme theoretical curves that can marginally fit the data. The values of the two parameters together also satisfy the necessary condition $\tau_m \approx \tau_r$, establishing the self-consistency of the slow reaction treatment.

Power-Law Dependence of the Rate on p_{NO_2}. Having determined the value of H_{NO_2} and k_1 using the slow reaction treatment based on second-order aqueous-phase kinetics and NO_2 diffusant, we now find it possible to examine the apparent reaction order of the observed rate with respect to p_{NO_2}. Qualitatively, since the slow reaction regime is

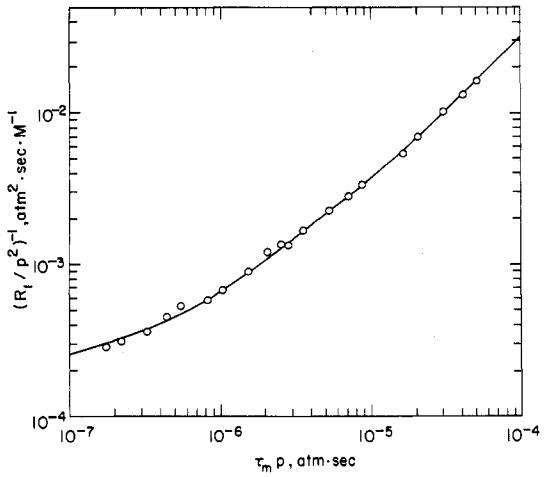

Figure 6. Dependence of the rate of reaction 1 upon characteristic mixing time, τ_m, plotted for a second-order reaction (eq 8).

intermediate between the phase-mixed and convective mass-transport controlled regimes, it is expected that the apparent reaction order for this regime be between 2 and 1, i.e., the orders for the two limiting regimes (Table II). Curve D of Figure 4 (representing eq 4) covering this regime shows not only an approximate slope of 3/2 but also a decrease in slope with increasing p_{NO_2} which is consistent with that expected as the regime changes from phase mixed to convective mass transport controlled with increasing p_{NO_2}.

Quantitatively, a theoretical prediction of the power-law dependence of the reaction rate can be made for a reaction of known order for each of the several regimes, making use of τ_m, k_1, and the Henry's law coefficient of the diffusant. For a second-order aqueous-phase reaction and NO_2 as the diffusing species, the rates of reaction for the three limiting regimes are as follows:[14]

A. phase-mixed (very slow reaction)

$$R_1 = k_1 H_{NO_2}^2 p_{NO_2}^2 \qquad p_{NO_2} \lesssim 8 \times 10^{-8} \text{ atm} \tag{9}$$

B. convective mass-transport limited

$$R_1 = \tfrac{1}{2} k_m H_{NO_2} p_{NO_2} \qquad 8.5 \times 10^{-6} \lesssim p_{NO_2} \lesssim 1.1 \times 10^{-4} \text{ atm} \tag{10}$$

C. diffusive mass-transport limited

$$R_1 = a(Dk_1/3)^{1/2}(H_{NO_2} p_{NO_2})^{3/2} \qquad p_{NO_2} \gtrsim 1.9 \times 10^{-3} \text{ atm} \tag{11}$$

where the criteria for the several regimes are derived from Table I for $\tau_m = 1.69$ s, corresponding to the mixing conditions of Figure 4. These equations are shown in Figure 4, lines A–C.

Line A (eq 9) for the phase-mixed regimes smoothly connects to the slow reaction regime data at the predicted p_{NO_2}. Line B (eq 10) calculated for the convective regime, which should be observed experimentally in the range $8.5 \times 10^{-6} \lesssim p_{NO_2} \lesssim 1.1 \times 10^{-4}$ atm, however, is seen to overlap with the data only in a rather narrow region, $8.0 \times 10^{-6} \leq p_{NO_2} \leq 3.1 \times 10^{-5}$ atm. At values of p_{NO_2} greater than this range the data exhibit positive deviation from line B and the slope of the log–log plot becomes greater than 1. A possible explanation for this deviation might be the onset of the transition to the molecular diffusive regime; however, as discussed below this would not appear to be the principal explanation for this departure.

In order to evaluate the rate of reaction 1 in the diffusive regime we found it necessary to know D, the diffusion

coefficient of dissolved NO_2, and a, the interfacial area per unit liquid volume characterizing the system. The former may be rather closely estimated from the semiempirical correlation of Wilke and Chang[19] as 2.0×10^{-5} cm^2 s^{-1}. Unfortunately the interfacial area is difficult to determine precisely for agitated-liquid reactors.[14] Nevertheless, one may provide a fairly narrow estimate of the possible range of this quantity based upon the observations of bank,[20] who has placed limits upon possible values of k_L (0.005–0.1 cm s^{-1}) and a (1–8 cm^{-1}). Consistent with the observed value $k_L a = k_m = 0.59$ s^{-1} the range of a characteristic of the present reactor may be further restricted to 5–8 cm^{-1}; this range in surface-to-volume ratio leads to a range in k_l evaluated by eq 11 (zone C in Figure 4). Zone C, which exhibits a slope of 3/2, is seen to cross curve B at $p_{NO_2} = 4 \times 10^{-4}$ atm; the onset of the purely diffusive mass transport regime would be expected at somewhat greater values of p_{NO_2}.

Although the above predictions are qualitatively exhibited by the data, examination of the measured rate in comparison to the predicted curve B suggests that the departure from B begins at partial pressures of NO_2 well below that inferred from the criterion given in Table I, and further the data appear to lie well above the values predicted by zone C. We thus raise the possibility of an alternative interpretation of this departure, namely, that of a shift in the diffusing species from the monomer NO_2 to the dimer N_2O_4. From Table III it is clear that the slope will become 2 when the diffusing species changes from NO_2 to N_2O_4 (for a true second-order reaction with respect to NO_2 or, equivalently, a first-order reaction with respect to N_2O_4). This slope of 2 would be expected for N_2O_4 as the diffusing species for all mass transport regimes.

To examine this interpretation, we made an estimate of the ratio of the concentration of N(IV) present as N_2O_4 to that present as NO_2, $N_{N_2O_4}/N_{NO_2}$, by the use of the aqueous-phase equilibrium constant K_A as determined by Grätzel et al.[8] Using the value $K_A = 6.5 \times 10^4$ M^{-1}, along with H_{NO_2} determined in the present study, we found that the ratio would be $\sim$0.1 at 2×10^{-4} atm, increasing at higher partial pressures. It therefore appears that the positive deviation from curve B is primarily due to the presence of N_2O_4 in solution in addition to the assumed NO_2, accounting for the onset of this departure at somewhat lower pressures than would be expected for NO_2 being the sole diffusing species. This discussion also serves to point out the risk in inferring the mass transport regime solely on the basis of the apparent reaction order with respect to p_{NO_2}.

Comparison with Other Work. The results of the present study may be compared directly to a limited number of previous studies and indirectly to a much larger body of work investigating the mechanism and rate of interaction of nitrogen oxides and water. Since the relation of the system under investigation here to the latter literature has recently been reviewed elsewhere,[13] we exclude from this discussion studies the results of which can be expressed only in terms of K_A and/or $H_{N_2O_4}$ and confine the present comparison to those studies whose results can be expressed in terms of H_{NO_2} and/or k_l. These studies are discussed below and summarized in Table V.

Among the directly relatable studies, the early work of Abel, Schmid, and co-workers[6] on the kinetics of decomposition and formation of nitrous acid represents a major contribution, in terms of both the insight afforded into the mechanism and kinetics of this reaction system and the

TABLE V: Comparison of Results

source	T, °C	k_l, M^{-1} s^{-1}	H_{NO_2}, M atm^{-1}	$H_{NO_2}{}^2 k_l$, M s^{-1} atm^{-2}
this work	22	1.0×10^8	7.0×10^{-3}	4.9×10^3
ref 6	22			4.7×10^3 [a]
ref 8	20	6.5×10^7		
ref 9	25	$4.7 \times 10^7 + 150$ s^{-1} [b]		
ref 10	25		4.0×10^{-2}	
ref 11	15	4.2×10^7	2.4×10^{-2}	
ref 4 (review)	25		$(1.1, 1.4) \times 10^{-2}$	

[a] Evaluated for 22 °C from original kinetic data (ref 6a) by employing temperature coefficient of ref 6c, and by employing modern value of equilibrium constant for $NO(g) + NO_2(g) + H_2O(l) = 2HNO_2(a)$ (ref 22). [b] First-order rate constant.

accuracy and precision of the measurements. In that study the kinetics of the forward and reverse reactions

$$3HNO_2 \underset{r}{\overset{f}{\rightleftharpoons}} 2\,NO(g) + H^+NO_3^- + H_2O$$

were determined and compared to the thermochemically determined equilibrium constant. The kinetic data may be interpreted in terms of a mechanism having the rate-determining step

$$2NO_2(a) + H_2O(l) \rightleftarrows HNO_2 + H^+NO_3^-$$

From the measured rate constant and also the equilibrium data for this system one obtains a rate constant for the overall reaction

$$2NO_2(g) + H_2O(l) \rightarrow HNO_2 + H^+NO_3^- \qquad (12)$$

as if this reaction were occurring under completely phase-mixed conditions, i.e., $[NO_2(a)] = H_{NO_2} p_{NO_2}$. Under such condition the rate of (12) is given by

$$R = k_{12} p_{NO_2}{}^2 \qquad (13)$$

The data of Abel et al.[6] together with modern thermochemical data[21] yield for k_{12} the values 4.06×10^3 and 4.25×10^3 M atm^{-2} s^{-1}, based, respectively, on the rates of nitrous acid formation and decomposition at 25 °C. The measured activation energy[6c] of the decomposition reaction permits evaluation of k_{12} at the temperature of the present study (22 °C), viz., 4.7×10^3 M atm^{-2} s^{-1}, where the value given represents the mean based on the decomposition and formation rates.

The results of the present study may be related to k_{12} by noting, from comparison of eq 9 and 13, that $k_{12} = H_{NO_2}{}^2 k_l$. Evaluation of k_{12} from the present data yields the value 4.9×10^3 M atm^{-2} s^{-1}, in agreement with the value derived from Abel and Schmid.[6]

The present results may also be compared directly to studies of the kinetics of aqueous-phase NO_2 prepared by pulse radiolysis[8] or flash photolysis.[9] The measurements of Grätzel et al., which exhibited mixed first- and second-order kinetics as the dominant N(IV) species changed from N_2O_4 to NO_2, yield $k_l = 6.5 \times 10^7$ M^{-1} s^{-1} at 20 °C, compared to the value of k_l obtained here, 1.0×10^8 M^{-1} s^{-1} at 22 °C.

In contrast to Grätzel et al.,[8] Treinin and Hayon[9] did not observe the transition from first- to second-order ki-

(19) C. R. Wilke and P. Chang, *Am. Inst. Chem. Eng. J.*, 1, 164 (1955).
(20) P. H. Calderbank, *Trans. Inst. Chem. Eng.*, 37, 173 (1959).
(21) D. D. Wagman, W. H. Evans, V. B. Parker, I. Halow, S. M. Bailey, and R. H. Schumm, *Natl. Bur. Stand. (U.S.), Tech. Note*, 270-3 (1968).

netics as [N(IV)] decreased. In order to account for the continued first-order loss of NO_2 the authors postulated the simultaneous occurrence of two reaction pathways, a path second order in NO_2 with $k_1 = 4.7 \times 10^7$, and a first-order path having rate $R_1 = k_{(1)}[NO_2]$ with $k_{(1)} = 1.5 \times 10^2$ s^{-1} at 25 °C. The present study is well suited to test for such a first-order process. Figure 5 permits the effective first-order rate constant to be evaluated from the slope–intercept ratio for each of the several partial pressures studied. The values obtained, 0.2–3 s^{-1}, are totally inconsistent with a first-order rate constant of the magnitude suggested by Treinin and Hayon. Furthermore, the power-law dependence of the rate with respect to p_{NO_2} did not show a slope of 1 in the log–log plot required for a first-order reaction, and therefore the contribution to reaction 1 of a first-order process with such a rate constant must be excluded. Indeed, as noted above, the present data are consistent with a second-order reaction down to the lowest partial pressures studied (1×10^{-7} atm).

The results of the present experiment may be compared also to previous direct measurements of the rate of uptake of NO_2 by water.[10,11] Andrew and Hanson,[10] interpreting the uptake of NO_2 to be in the convective regime at the lowest partial pressures employed (1.9×10^{-4}–3.7×10^{-4} atm), reported $H_{NO_2} = 4 \times 10^{-2}$ M atm^{-1} (25 °C). Recently, Komiyama and Inoue[11] have reported apparent orders for reaction 1 of 1, 3/2, and 2, increasing with increasing p_{NO_2}. The first-order data (1.2×10^{-5}–2.4×10^{-5} atm), interpreted as convectively controlled uptake with NO_2 being the diffusant species (eq 10), yielded $H_{NO_2} = 2.4 \times 10^{-2}$ atm (15 °C). The 3/2-order data (3.4×10^{-5}–2.9×10^{-4} atm) were interpreted as diffusive mass transport, again with NO_2 as the diffusant species (eq 11). This treatment yielded (for D_{NO_2} taken as 1.0×10^{-5} cm^2 s^{-1}) $H_{NO_2}{}^{3/2}k_1{}^{1/2} = 23$ M $atm^{-3/2}$ $s^{-1/2}$; this result, in conjunction with their value of H_{NO_2} yielded, $k_1 = 4.2 \times 10^7$ M^{-1} s^{-1}. Finally, the data of the second-order regime (5×10^{-4}–1.3×10^{-3} atm) were interpreted as diffusive mass transport with N_2O_4 as the diffusant species. That treatment, in conjunction with H_{NO_2} and k_1 permits, by an argument that need not be repeated here, evaluation of the equilibrium constant K_A, for which the value 7.6×10^4 M^{-1} was reported.

It is instructive to examine the interpretation of Komiyama and Inoue for self-consistency. In particular using their values of H_{NO_2} and K_A we find that over the pressure range yielding the apparent 3/2 order (which was interpreted as diffusion-controlled reaction of NO_2 diffusant) the fraction of N(IV) present as N_2O_4 ranged from 11 to 50%. This finding contradicts the assumption that NO_2 was the sole diffusing species and establishes that their interpretation leading to k_1 and K_A cannot be correct.

A similar examination may be made of the first-order regime, for assumed value of K_A. If we take the value of Grätzel et al. (6.5×10^4 M^{-1}) it would appear that in the partial pressure range of Andrew and Hanson the fraction of N(IV) present as N_2O_4 was 50–65%, thus resulting in too great a value of H_{NO_2}. The same analysis applied to the first-order regime of Komiyama and Inoue indicates only 4–7% N_2O_4. Thus it would not appear that their value of H_{NO_2} can be excluded on these ground. We are therefore unable to account for the discrepancy between their value of H_{NO_2} and that obtained here, although we would point out that their result is based upon only two measurements at the extreme low pressure end of their experimental range (1.2×10^{-5}–2.4×10^{-5} atm).

Finally, we would note that the study of the reactive uptake of NO_2 in the slow reaction regime as has been reported here appears to afford a more direct interpretation than is available in approaches previously employed. First, by working in the slow reaction regime it is necessary only to know the convective mixing rate k_m ($\equiv k_L a$) characteristic of the reactor and not the interfacial area as in the case with studies in the diffusive regime. This has the advantage that k_m is readily measured, whereas there is no convenient method for determination of a.[14] Secondly, by working in the slow reaction regime one may determine both elementary constants, i.e., the Henry's law coefficient and the aqueous-phase rate constant. Third, in the case of reactions of NO_2, working at low partial pressure has the advantage of avoiding any complication arising from participation of the dimer in the mass-transport process.

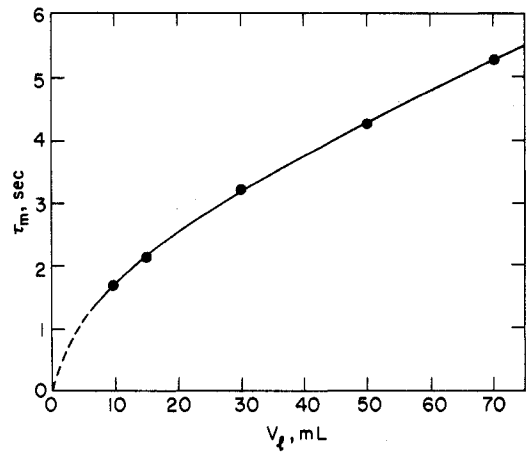

Figure 7. Dependence of the characteristic mixing time (τ_m) of the gas–liquid reaction cell upon liquid volume, at total flow rate = 2.0 L/min. Points represent averages of four or more measurements.

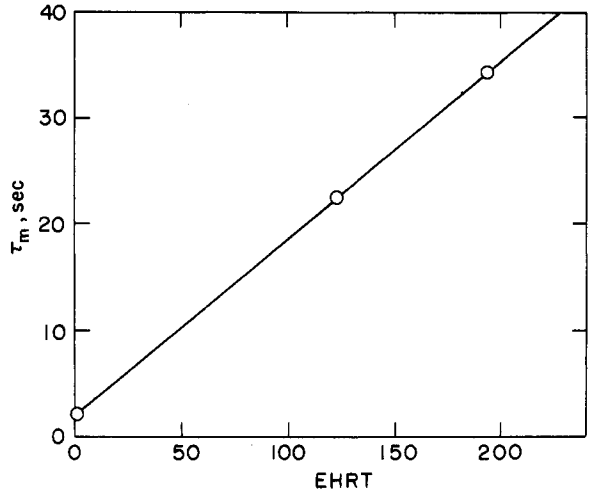

Figure 8. Dependence of the characteristic mixing time, τ_m, upon the solubility of the dissolving gas. See Appendix for the definition of E. Points represent averages of four or more measurements.

Summary

The reactive dissolution of NO_2 was studied over the NO_2 partial pressure range extending downward from 8×10^{-4} to 1×10^{-7} atm. The stoichiometry of the reaction is $2NO_2(g) + H_2O(l) = 2H^+ + NO_3^- + NO_2^-$. The kinetics over the entire range were consistent with a second-order aqueous-phase reaction coupled to mass-transport process. Measurements at the lower partial pressures were interpreted according to the theory of slow reactions as governed by chemical reaction and convective mass transport, yielding values for the Henry's law coefficient of NO_2 of $H_{NO_2} = 7.0 \times 10^{-3}$ M atm^{-1}, and the second-order aqueous-phase reaction constant of $k_1 = 1.0 \times 10^8$ M^{-1} s^{-1}.

Acknowledgment. This work was supported in part by the High Altitude Pollution Program of the Office of Environment and Energy, Federal Aviation Administration, and was performed under the auspices of the United States Department of Energy under Contract No. DE-AC02-76CH00016.

Appendix. Characterization of Mixing Rate

As emphasized in the text and elsewhere,[14] the characterization of the rate of convective mixing k_m of the reactor is crucial to the interpretation of kinetic studies of gas–liquid reactions in the slow reaction limit. In order to determine this mixing rate for our reactor we have measured this quantity for CO_2. As shown below CO_2 serves as a suitable model for the reagent gas of interest here, NO_2, and thus k_m as determined with CO_2 may be employed in the interpretation of the NO_2 kinetics.

The first-order kinetics of CO_2 uptake into water[14]

$$[CO_2]_t = [CO_2]_\infty(1 - e^{-k_m t}) \tag{A1}$$

can be followed by the conductivity change of the solution due to the dissociation process

$$CO_2 + H_2O \rightleftarrows H^+ + HCO_3^- \tag{A2}$$

Because the species being monitored is HCO_3^-, rather than CO_2, k_m is determined from the asymptotic approach to the equilibrium conductivity

$$\kappa_t = \kappa_\infty(1 - \tfrac{1}{2}e^{-k_m t}) \tag{A3}$$

where κ is the conductivity and t and ∞ denote time = t and = ∞.

To begin the experiment, N_2 and CO_2 flows were first adjusted so that, when switched into the main path, each would flow at the same rate. Before starting the measurement, N_2 was flowing through the cell and CO_2 was flowing into exhaust through valve E1 and a back-pressure regulator, which maintained the same upstream pressure of CO_2 as that of N_2. When actuated, electric-solenoid-controlled three-way valves E1 and E2, coupled electrically, were switched such that gas flow routes were alternated, now with CO_2 flowing into the cell and N_2 into the air. The conductivity of the solution was recorded as a function of time on an x–y plotter (Varian, Model F-80). The rate of uptake was studied as a function of liquid volume in the reaction cell for a fixed gas flow and the results are shown in Figure 7.

Liquid-Side Resistance and CO_2 as a Model. The rate coefficient, k_m, measured for the CO_2 dissolution is a product of K_L, the overall mass transfer coefficient, and a, the interfacial area per unit volume of solution.[14] The latter quantity depends only upon the physical mixing of the system, but K_L depends upon both the physical mixing and the nature of the solute. The overall mass transfer coefficient is related to the liquid-side and gas-side mass transfer coefficient by

$$\frac{1}{K_L} = \frac{1}{k_L} + \frac{EHRT}{k_G} \tag{A4}$$

where **R** is the gas-law constant, T the absolute temperature, H is the Henry's law coefficient of the gas, and E is the enhancement factor, defined as the ratio of the concentration of total dissolved substance to that of the physically dissolved gas molecules. The chemical species must be formed from the diffusing species in a characteristic time much shorter than that of mixing in order to be included in the total substance. For SO_2, the enhancement factor is given as

$$E = \frac{[SO_2] + [HSO_3^-] + [SO_3^{2-}]}{[SO_2]}$$

since the dissociation time constant of SO_2 is much shorter than the molecular diffusion time constant.[22]

To determine the relative importance of the two terms one can plot τ_m (defined as $1/K_L a$) as a function of $EHRT$; from such a plot $1/k_L a$ and $1/k_G a$ can be obtained as the intercept and the slope. The dependence of τ_m on $EHRT$ is given in Figure 8; the point for $EHRT = 1.0$ was for CO_2 and the points at higher $EHRT$ were for SO_2 studied at $p_{SO_2} = 1.63 \times 10^{-3}$ and 5.11×10^{-4} atm. The fact that both H and K_1 (the dissociation constant for $SO_2 + H_2O \rightleftarrows H^+ + HSO_3^-$) are well known for SO_2 (also for CO_2) made $EHRT$ values readily available.

The straight line in Figure 8 yielded ratio of $k_G/k_L = 12$ indicating that gas-phase resistance is far smaller than that of liquid-phase in the gas–liquid reactor employed in this study. The use of CO_2 as a model for NO_2 in the mixing characterization is therefore appropriate, provided that $EHRT$ for NO_2 is at least as small as that for CO_2, which is true for NO_2 in the slow reaction regime.

(22) S. E. Schwartz and J. E. Freiberg, *Atmos. Environ.*, in press.